Decentralized Model Predictive Control for Platooning: Enhancing Human-Driver Collaboration

Justin M. Kennedy, *Member, IEEE*, Lixin Yang, Daniel E. Quevedo, *Fellow, IEEE*, Falko Dressler, *Fellow, IEEE*

***Abstract*—Recent advances in cooperative adaptive cruise control have demonstrated the potential for vehicle platooning to revolutionize road transportation through enhanced safety, reduced congestion, and improved energy efficiency. While autonomous vehicle technology continues to evolve rapidly, current regulatory frameworks and safety considerations necessitate the human driver supervision. This creates a unique challenge in developing control systems that can effectively balance autonomous operation with human intervention. To enhance the human-driver collaboration with autonomous vehicle platooning, in this paper, we present a novel decentralized model predictive control framework that explicitly incorporates human-driver interaction while maintaining desired inter-vehicle distances and velocities in platoon formations. This framework employs a distributed architecture where each vehicle operates independently and exchanges local measurements through vehicle-to-vehicle communication. To overcome the inherent unreliability of wireless communications in real-world scenarios, we develop a robust distributed state estimation strategy. This approach enables each vehicle to combine local sensor measurements with received data to construct accurate estimates of the full platoon state. Based on these estimates, vehicles compute optimal control actions locally while achieving performance comparable to an ideal centralized controller with perfect communication. Through extensive Plexe simulations, we demonstrate that the proposed decentralized model predictive controller achieves comparable performance to the ideal centralized case, even under partial state information and communication constraints.**

***Index Terms*—Platooning, Cooperative Adaptive Cruise Control, Model-Predictive Control, Human-Driver Interaction, Hybridized Cyber-Physical Systems.**

I. Introduction

Autonomous vehicle platooning involves a series of autonomous vehicles traveling closely together in a coordinated manner, utilizing advanced communication and control technologies to enhance road transportation efficiency [1]–[3]. This approach offers several benefits, including improved efficiency, safety, and fuel economy, making it a promising solution for practical applications. One notable application is truck platooning, where multiple trucks travel together to reduce fuel consumption and enhance delivery efficiency [4]. Similarly, autonomous buses can form platoons to provide efficient and reliable public transport services [5]. Significant research efforts have been dedicated to developing control algorithms, spacing policies, communication technologies, information flows, and stability to disturbances [6]–[9].

An autonomous vehicle platoon can be formed of a sequence of vehicles using Adaptive Cruise Control (ACC), which maintains a safe distance from the vehicle ahead [10]. ACC employs sensors such as radar, LIDAR, or cameras to detect the distance to, and relative speed of, the preceding vehicle. Utilising the distance and speed information, ACC automatically adjusts the vehicle's speed by controlling the throttle and brakes to maintain a preset following distance. A platoon of vehicles utilising ACC are known to be unstable in a string stability sense [11], leading to ghost traffic jams. To ensure platoon stability, either a large, velocity-based inter-vehicle distance is required using a headway time [8], or additional information beyond the state of the preceding vehicle [12] is needed. An advanced version of ACC, Cooperative Adaptive Cruise Control (CACC), incorporates Vehicle to-Vehicle (V2V) or Vehicle to-Everything (V2X) communication to enhance coordination between multiple vehicles [13], see Figure 1. Vehicles equipped with CACC communicate with each other using Dedicated Short-Range Communication (DSRC) or cellular networks to exchange real-time data [14]. By sharing information, CACC systems can anticipate the actions of other vehicles in the platoon, resulting in smoother and more synchronized speed adjustments [15]. The cooperative aspect of CACC enables more precise and timely adjustments, reducing the likelihood of collisions and improving overall road safety.

However, current real-world deployments of CACC systems remain in a transition phase, where full automation is not universally available or trusted. Human drivers may choose to engage or disengage automation at any position in the platoon [16], [17]. Such behavior is common in scenarios involving ride-hailing fleets [18], manually operated logistics vehicles [19], or level-3 autonomy where the system frequently requests human takeover [20]. In these cases, platoon formation must tolerate partial human intervention without sacrificing safety or stability [21]. Such human interventions, particularly emergency maneuvers, create significant challenges for platoon stability and safety. Without proper system design, a sudden braking action by human drivers could result in collisions with following vehicles that lack immediate access to information about the human driver's control actions. Although CACC systems incorporate collision avoidance features via onboard sensors, these typically rely on reactive proximity sensing. In

This work was supported in part by the project NICCI2 funded by the German Research Foundation (DFG) under grant numbers DR 639/23-2 and QU 437/1-2. (*Corresponding author: Lixin Yang*)

Justin M. Kennedy is with the School of Electrical Engineering and Robotics, Queensland University of Technology, Brisbane, QLD 4000, Australia (e-mail: j12.kennedy@qut.edu.au).

Lixin Yang is with the Department of Electrical and Computer Engineering, National University of Singapore, Singapore (email: lixin.yang@nus.edu.sg).

Daniel E. Quevedo is with the School of Electrical and Computer Engineering, The University of Sydney, Sydney, NSW 2006, Australia (e-mail: daniel.quevedo@sydney.edu.au).

Falko Dressler is with the School of Electrical Engineering and Computer Science, TU Berlin, 10623 Berlin, Germany (e-mail: dressler@ccs-labs.org).

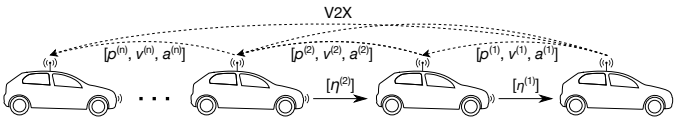

Figure 1. CACC concept: a platoon controller regulates the velocity and inter-vehicle distances utilizing the vehicles' position p, velocity v, and acceleration a, exchanged via inter-vehicle communications.

situations where a human driver within the platoon executes a sudden maneuver without prior signaling (e.g., emergency braking without V2V messaging), the response latency can compromise safety, particularly at short inter-vehicle gaps [22]. By explicitly integrating human behavior into the control loop, our framework aims to proactively adjust the actions of ego vehicles, and mitigate risks beyond what purely sensor-driven systems can address. In contrast to traditional mixed traffic flow, where automated and human-driven vehicles are interleaved without coordination [23], [24], we consider a semi-cooperative platoon framework. Specifically, certain vehicles within the formation may be human-controlled but still participate in shared estimation and information exchange. This setup introduces unique challenges in predicting human driver actions and maintaining platoon formation.

Effective platoon control requires sophisticated control strategies that can handle both autonomous operations and human interventions while maintaining safety and performance. Among various control approaches, including Linear Quadratic Regulator (LQR) [25], Proportional Integral Derivative (PID) [26], H-infinity [27], and sliding mode control [28], Model Predictive Control (MPC) stands out for its ability to explicitly incorporate safety constraints and vehicle dynamics [29]–[31]. MPC-based CACC designs are particularly advantageous as they can directly account for road speed limits, minimum safe inter-vehicle distances, and actuation constraints while optimizing future control actions. However, the implementation architecture of MPC controllers significantly impacts their practical viability. While centralized MPC approaches can achieve optimal performance by considering the entire platoon state, they face substantial challenges in real-world deployment due to communication reliability issues and computational scalability limitations [32]. These challenges become particularly acute when human driver interventions must be accommodated, as the central controller requires immediate access to all vehicle states and human control inputs.

To address these practical limitations, our work develops a decentralized MPC framework where each vehicle independently computes its control actions based on local information and limited communication with neighboring vehicles. This decentralized approach offers several key advantages: (1) reduced communication overhead and enhanced robustness to network failures, (2) improved scalability for larger platoons, and (3) faster response to local disturbances, including human driver interventions. In our framework, each vehicle maintains a local estimate of the platoon state through a combination of onboard sensors and V2V communication, enabling it to compute control actions that maintain platoon stability even during human interventions or communication disruptions. This distributed computation approach eliminates the single point of failure inherent in centralized systems while maintaining comparable performance through careful coordination of local control actions. Our design specifically accounts for the practical challenges of human-driver interaction, unreliable inter-vehicle communication, and the need for real-time response to changing traffic conditions. Unlike traditional decentralized control, where each vehicle computes only its own control action, our approach allows each vehicle to compute an augmented control vector for the entire platoon, applying only the portion relevant to itself. Controllers are embedded within each vehicle and operate exclusively on local information obtained from the vehicle itself and its immediate neighbors. While this method extends beyond standard decentralized control paradigms, it remains decentralized in nature, offering a robust and scalable solution for modern platooning systems.

Motivated by these challenges, we present a comprehensive framework for decentralized MPC design that effectively integrates human-driver interaction in autonomous vehicle platooning. Our main contributions are:

1) We propose a decentralized MPC framework for vehicle platooning that explicitly accounts for both unreliable V2V communication and partial human driver participation within the platoon. Unlike existing works that assume fully autonomous vehicles, our approach enables semi-cooperative platoon operation where certain vehicles may temporarily fall under human control.
2) A novel multi-rate measurement fusion and state estimation scheme is developed to handle asynchronous and delayed information sharing among vehicles. By combining locally sensed and intermittently received data, each vehicle independently reconstructs the global platoon state and computes near-optimal control actions without requiring centralized coordination.
3) We conduct a comprehensive implementation and evaluation using the Plexe simulation platform under realistic DSRC-based communication constraints [33]. Our results demonstrate that the proposed method maintains stable platoon operation across heterogeneous vehicle dynamics and mixed human-autonomous participation, which surpasses the performance limitations observed in prior decentralized approaches [34].

The structure of this paper is as follows: Section II outlines the system dynamics involving human-driver interaction, along with sensor measurements and inter-vehicle communication. Section III formulates the problem addressed in this work. Section IV presents the distributed platoon state estimation framework, while Section V details the decentralized platoon control design. Section VI assesses the performance through numerical experiments. Finally, Section VII provides the conclusion.

Notations: Let $p_k^{(i)}$, $v_k^{(i)}$, and $a_k^{(i)}$ denote the position [m], velocity [m/s], and acceleration [m/s^2] of vehicle i, respectively. The control input $u_k^{(i)}$ [m/s^2] represents the desired acceleration applied to vehicle i. The state vector of vehicle i is defined as $x_k^{(i)} = [p_k^{(i)}, v_k^{(i)}, a_k^{(i)}]^\top$, and the augmented state vector of the entire platoon is $X_k = [x_k^{(1)\top}, \ldots, x_k^{(M)\top}]^\top$. The control input vector is $U_k = [u_k^{(1)}, \ldots, u_k^{(M)}]^\top$, with change in control action

$\Delta U_k = U_k - U_{k-1}$. Each vehicle obtains a noisy measurement vector $y_k^{(i)}$, and forms a local estimate of the full platoon state denoted by $\hat{X}_k^{(j)}$. The diagonal matrices α_k and $\bar{\alpha}_k$ serve as indicators for vehicles under autonomous control or human override, respectively. The main control sampling interval is Δ_t, while δ_t denotes the finer sampling interval used in the multi-rate measurement fusion.

II. Physical System

A. Vehicle Dynamics

For the longitudinal motion of a single vehicle i, we consider the commonly utilized linear dynamics from [28]. Let us define the state as $p^{(i)}$ [m] as a point at the front bumper, $v^{(i)}$ [m/s] the velocity, $a^{(i)}$ [m/s^2] acceleration, and $u^{(i)}$ [m/s^2] control input or desired acceleration. The time derivative of each state is $\dot{p}^{(i)} = v^{(i)}$, $\dot{v}^{(i)} = a^{(i)}$, and

$$\dot{a}^{(i)} = -\frac{1}{\tau_i} a^{(i)} + \frac{1}{\tau_i} u^{(i)}$$

where τ_i [s] is the mechanical actuation lag. The mechanical actuation lag represents the time delays resulting from moving components in the engine and braking systems. The time discretization with constant sampling interval Δ_t [s/sample] for a single vehicle is given in [35]. We define t [s] as time and k [samples] as the discrete time index with the relation $t = k\Delta_t + t_0$ where t_0 [s] is an initial offset. Denote the state of vehicle i as $x_k^{(i)} = [p_k^{(i)}, v_k^{(i)}, a_k^{(i)}]^\top$. The dynamics of each vehicle are given by

$$x_{k+1}^{(i)} = A^{(i)} x_k^{(i)} + B^{(i)} u_k^{(i)} + w_k^i \tag{1}$$

where $A^{(i)}$ and $B^{(i)}$ are the system matrix and control matrix, respectively, as provided in [35]. The term w_k^i represents i.i.d. zero-mean Gaussian noise with distribution $w_k^i \sim \mathcal{N}(0, \mathcal{W}^{(i)})$.

B. Platoon Architecture

Following [25], [35], [36] and [37], we will implement decentralized control for the platoon by considering a combined model. For M vehicles in a straight line led by vehicle 1 and tailed by vehicle M, we define the augmented platoon state as

$$X_k = [p_k^{(1)}, \ldots, p_k^{(M)}, v_k^{(1)}, \ldots, v_k^{(M)}, a_k^{(1)}, \ldots, a_k^{(M)}]^\mathsf{T} \tag{2}$$

and the augmented control vector as $U_k = [u_k^{(1)}, \ldots, u_k^{(M)}]^\mathsf{T}$ with control input $u_k^{(i)}$. Based on (1), the dynamics of the platoon is then given by

$$X_{k+1} = A_M X_k + B_M U_k + W_k \tag{3}$$

where A_M and B_M are block diagonal matrices of the collection of single-vehicle dynamics and control input matrices given in [35], W_k is a vector of the i.i.d. process noise acting on each vehicle which can be modeled as a zero-mean Gaussian process $W_k \sim \mathcal{N}(0, \mathcal{W})$, and $U_k = U_{k-1} + \Delta U_k$ where $\Delta U_k = [\Delta u_k^{(1)}, \ldots, \Delta u_k^{(M)}]^\mathsf{T}$ and $\Delta u_k^{(i)}$ is the change in control action for vehicle i. We consider that each vehicle in the platoon can take a different mechanical actuation lag resulting in a so-called heterogeneous platoon. Using the state X_k and previous control action U_{k-1}, the MPC design computes the change in control action ΔU_k [35].

In our decentralized MPC design, instead of directly computing the control action U_k, we compute the change in control action ΔU_k. This approach is adopted to achieve smoother control inputs, which are essential for maintaining passenger comfort and preventing abrupt maneuvers that could destabilize the platoon. Furthermore, vehicles have physical constraints, such as maximum acceleration and deceleration rates. By focusing on ΔU_k, it becomes convenient to design controllers that adhere to these constraints, ensuring safe and feasible operation.

C. Inclusion of Human Drivers

Due to legal requirements [38], a responsible human driver must be present in the vehicle at all times when autonomous vehicles are on the road. The human driver's authority typically supersedes that of the vehicle's controller. This work, therefore, considers scenarios where the human driver may override the platoon controller to operate the vehicle manually. To maintain platoon formation, we desire that the platoon controller reconfigures to the temporary interruption by a human driver. We assume that the human driver is solely focused on the state of their own vehicle, does not interact with any other vehicles in the platoon, and issues control actions that are consistent with physical (engine limit) and legal (road speed limit) constraints.

Consider a vehicle ℓ that is temporarily under human driver control and not under platoon control. Although the vehicle remains physically within the platoon, it follows the human driver's commands rather than the platoon controller. Specifically, it will experience a change in control action $\Delta \mathrm{u}_k^{(\ell)}$ from the human driver replacing the platoon control $\Delta u_k^{(\ell)}$ such that the control action is $u_k^{(\ell)} = u_{k-1}^{(\ell)} + \Delta \mathrm{u}_k^{(\ell)}$. For ease of notation, we modify the platoon control action in Equation (3) with a switch

$$U_k = U_{k-1} + \alpha_k \Delta U_k + \bar{\alpha}_k \Delta \mathcal{U}_k \tag{4}$$

where $\Delta \mathcal{U}_k$ is the control action applied from a human driver. The binary switch α_k is a diagonal square matrix of size M that takes ones on the diagonal for the vehicles controlled by the platoon and zero in the i,ith element when vehicle i is not controlled by the platoon controller, and $\bar{\alpha}_k = I_M - \alpha_k$. When the platoon is controlled by the controller, $\alpha_k \equiv I_M$ and $\bar{\alpha}_k \equiv 0_M$, and Equation (4) reduces to Equation (3). The dynamics of the platoon Equation (3) are now

$$X_{k+1} = A_M X_k + B_M U_{k-1} + B_M \alpha_k \Delta U_k + B_M \bar{\alpha}_k \Delta \mathcal{U}_k. \tag{5}$$

In the centralized design, the controller knows the applied control at time $k-1$ and is aware if every vehicle has utilized the centralized platoon controller or an alternative control value. In the present work, the applied control action is shared with state measurements via inter-vehicle communications, discussed below. As such, the switch α_k is known to the controller at time k. If a vehicle has temporarily left the platoon, we assume that the vehicle will continue to be human controlled until informed otherwise, and α_k is constant.

D. Sensor Measurements

We consider that there are at least five sensors onboard a single vehicle, see [6], [39]. Utilizing Global Navigation Satellite System (GNSS) and local sensors, the vehicle measure its own position $p_k^{(i)}$, velocity $v_k^{(i)}$, and acceleration $a_k^{(i)}$. Many modern consumer vehicles are equipped with forward facing radars for ACC [40]. These radars detect a vehicle in front then measure the forward inter-vehicle distance $p_k^{(i)} - p_k^{(i-1)}$. Future connected vehicles will use the same radar technology at the rear of a vehicle to detect and measure the backward inter-vehicle distance $p_k^{(i)} - p_k^{(i+1)}$.

Consider a vehicle i in the middle of the platoon for $i = 2, \ldots, M-1$ then the measurement at time k can be written as

$$\tilde{y}_k^{(i)} = [p_k^{(i)}, v_k^{(i)}, a_k^{(i)}, p_k^{(i)} - p_k^{(i-1)}, p_k^{(i)} - p_k^{(i+1)}]^\mathsf{T}.$$

As the lead vehicle 1 does not follow any vehicles then its measurement is $\tilde{y}_k^{(1)} = [p_k^{(i)}, v_k^{(i)}, a_k^{(i)}, p_k^{(i)} - p_k^{(i+1)}]^\mathsf{T}$, and as the final vehicle M is not followed by any vehicles, thus $\tilde{y}_k^{(M)} = [p_k^{(i)}, v_k^{(i)}, a_k^{(i)}, p_k^{(i)} - p_k^{(i-1)}]^\mathsf{T}$. Each of the vehicles' measurements would be affected by inaccuracies in the sensor [41]. This measurement error can be represented by the linear addition of a noise term $\mathfrak{v}_k^{(i)}$ modeled as zero mean Gaussian distribution with covariance $\mathcal{R}_i$. The noisy measurement available from the set of sensors at each vehicle i is $y_k^{(i)} = \tilde{y}_k^{(i)} + \mathfrak{v}_k^{(i)}$.

The measurements for vehicle i at time k can be written as a linear function of the state Equation (2) as $y_k^{(i)} = C_i X_k + \mathfrak{v}_k^{(i)}$, where the measurement matrix C_i for intermediate vehicle i for $i = 2, \ldots, M-1$ is a zero matrix of size 5 by $3M$ with 1 in position $(1, i)$, $(2, M+i)$, $(3, 2M+i)$, $(4, i)$ and $(5, i)$, and -1 in position $(4, i-1)$ and $(5, i+1)$, i.e.,

$$C_i = \begin{bmatrix} 0 & \cdots & 0 & 1 & 0 & \cdots & 0 & 0 & \cdots & 0 & 0 \\ 0 & \cdots & 0 & 0 & 0 & \cdots & 1 & 0 & \cdots & 0 & 0 \\ 0 & \cdots & 0 & 0 & 0 & \cdots & 0 & 0 & \cdots & 1 & 0 \\ 0 & \cdots & -1 & 1 & 0 & \cdots & 0 & 0 & \cdots & 0 & 0 \\ 0 & \cdots & 0 & 1 & -1 & \cdots & 0 & 0 & \cdots & 0 & 0 \end{bmatrix}_{5 \times 3M}$$

Similarly, for the lead vehicle, C_1 is a matrix of size 4 by $3M$ with 1 in position $(1, 1)$, $(2, M+1)$, $(3, 2M+1)$, and $(4, 1)$ and -1 in position $(4, 2)$, and for the tail vehicle, C_M a matrix of size 4 by $3M$ with 1 in position $(1, M)$, $(2, 2M)$, $(3, 3M)$, and $(4, M)$ and -1 in position $(4, M-1)$.

The full set of measurements available to the platoon is defined as $\tilde{y}_k \triangleq [(\tilde{y}_k^{(1)})^\mathsf{T}, \ldots, (\tilde{y}_k^{(M)})^\mathsf{T}]^\mathsf{T} = CX_k$ where $C = [C_1^\mathsf{T}, \ldots, C_M^\mathsf{T}]^\mathsf{T}$. In this context, $\tilde{y}_k$ represents the collective measurements from all vehicles in the platoon, and X_k denotes the state of the platoon at time k. The matrix C combines the individual measurement matrices C_i of each vehicle into a single comprehensive measurement matrix. Consider the platoon dynamics A_M and the full measurement matrix C. Given these full measurements $\tilde{y}_k$, the platoon state X_k is fully observable. This implies that with the complete set of measurements, one can construct an accurate estimate of the entire platoon state [41]. However, in practice, each vehicle i can only has access to its own measurements $y_k^{(i)}$. Consequently, consider the platoon dynamics A_M and a measurement matrix C_i for each vehicle i. The full platoon state X_k is not fully observable. This lack of full observability means that an individual vehicle cannot compute an accurate estimate of the entire platoon state using only its own measurements.

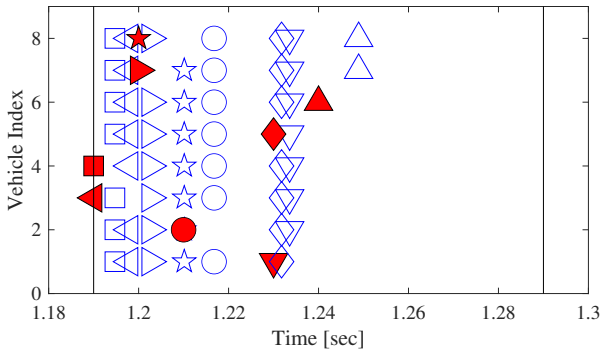

Figure 2. Plexe Experiment: packet transmission schedule and receipt delays. Sampling window is denoted with vertical black lines. Open symbol indicates packet receipt in the line of the vehicle received. Colored red packet is transmission time. Symbol indicates vehicle index: upside down triangle, circle, left-triangle, square, diamond, triangle, right-triangle, star, from vehicle 1 to-8, respectively. Note that the transmission from vehicle 6 is only received by vehicle 7 and-8.

To address this, inter-vehicle communication is essential. Vehicles must share their partial state measurements with one another to enable the decentralized platoon controller to function effectively. By exchanging measurement information, vehicles can collectively reconstruct the full state X_k and thus implement the decentralized control strategy. In the subsequent sections, we will discuss an inter-vehicle communication technology that facilitates this information sharing. We will also present a practical decentralized implementation of the platoon control, allowing vehicles to operate collaboratively while maintaining the benefits of centralized control.

E. Inter-Vehicle Communication

In our approach, we utilize V2V communication to exchange information between vehicles. Alternative approaches include combining and relaying transmissions [42], or using infrastructure in a V2X design, see [43] for a computational approach. Vehicles communicate by means of IEEE 802.11p-based DSRC in the 5 GHz band. They periodically exchange platooning information by transmitting beacons at a constant frequency of 10 Hz (*static beaconing*). Hence, new beacon packets are being generated at a constant interval of 100 ms. After channel access Carrier Sensing Multiple Access with Collision Avoidance (CSMA/CA), which can introduce random delay, the packets are transmitted as broadcast. In other words, each vehicle transmits its measurements to all other vehicles within the platooning. The transmitted wireless signal is impacted by propagation delay as well as attenuation. Thus, packets can be either received successfully or dropped due to bit errors, interference, or generally low Signal-to-Noise Ratio (SNR). Overall, the probability of a successful packet transmission is binary while its delay is continuous (> 0).

In order to demonstrate the V2X communication for exchanging platooning information, we show a short time-span from a exemplary simulation run with Plexe [33] for a single sampling

Table I
SIMULATION PARAMETERS FOR V2X COMMUNICATION

Parameter	Value
Beacon size	200 Byte
Beaconing approach	Constant 100 ms interval
MAC model	IEEE 802.11p
Access Category (AC)	AC_VI
PHY model	IEEE 802.11p
Frequency f	5.89 GHz
Bandwith	10 MHz
Path loss model	Free space ($\alpha = 2.0$)
Bitrate	6 Mbit/s (QPSK $R = \frac{1}{2}$)
Bitrate interfering vehicles	3 Mbit/s (QPSK $R = \frac{1}{2}$)
Maximum transmit power	20 dBm = 100 mW
CCA threshold	−65 dBm
Sensitivity	−94 dBm
Thermal noise	−95 dBm

period in Figure 2. We simulate a platoon with 8 vehicles that is driving with constant speed on the right-most lane of a 4-lane freeway. The platoon is driving with leader-follower control by using a CACC with a constant spacing policy on every vehicle. It is utilizing regular platoon beacons from the leading and front corresponding vehicle, which are transmitted by the platoon members via the aforementioned communication technology. Additionally, we placed 100 non-platooning vehicles at a uniformly distributed fixed location on the other lanes of the freeway. These vehicles are also periodically transmitting beacons, in order to generate background traffic and interference. For every successfully received message, we measure a collection of metrics at the corresponding receiving vehicles. Further details of our simulation setup are listed in Table I. In Figure 2, we can observe that the channel access is delaying packets and some transmissions are not successful.

Remark 1. *While the current implementation and evaluation are conducted via Plexe simulations, real-world experimentation remains an essential for future work. In particular, integrating the proposed framework with modern communication infrastructures such as 5G-V2X would further enhance the reliability and responsiveness of decentralized platoon control. Future works will focus on transitioning from simulation to experiments to validate the estimation and control strategies under real-world dynamics and communication environments.*

III. PROBLEM FORMULATION

We consider the platoon control problem where a platoon of vehicles stays together, including in the situation of a human driver taking temporary control of their vehicle. We desire to control the entire platoon to reach a target velocity of v_d [m/s] with the desired distance between vehicle i and its immediate predecessor vehicle $(i-1)$ given by

$$\bar{d}_k^{(i)} \triangleq d_i + h_k^{(i)} v_k^{(i)} = l_{i-1} + r_i + h_k^{(i)} v_k^{(i)} \tag{6}$$

where $d_i = l_{i-1} + r_i$ is the constant inter-vehicle distance, l_{i-1} [m] is the length of vehicle $(i-1)$, r_i [m] the desired standstill distance in front of vehicle i, and $h_k^{(i)}$ [s] the desired headway time. The headway time quantifies the distance to the preceding vehicle at the current velocity. The desired standstill distance r_i and headway time $h_k^{(i)}$ are vehicle specific and can be chosen by the respective driver, whereas the desired velocity is platoon specified. We also denote the individual desired headway as time-dependent, as we allow the human occupants of the vehicle to increase or decrease their inter-vehicle distance.

Additionally, we desire to ensure the following constraints for all vehicles $i = 1, \dots, M$:

C1: $p^{(i-1)} - p^{(i)} \geq d_{\text{min}}$, minimum safe distance between vehicles to ensure that no vehicle impacts its predecessor,
C2: $p^{(i-1)} - p^{(i)} \leq d_{\text{max}}$ maximum distance between vehicles to ensure communications are maintained,
C3: $v_{\text{min}} \leq v^{(i)}$, minimum velocity set to zero so that no vehicle in the platoon reverses on the road,
C4: $v^{(i)} \leq v_{\text{max}}$, maximum velocity chosen based on the road speed limit, or the performance limitation of a vehicle,
C5: $a_{\text{min}} \leq a^{(i)}$, minimum acceleration bounded based on the performance of the braking systems, and
C6: $a^{(i)} \leq a_{\text{max}}$, maximum acceleration chosen based on the engine performance of the vehicles.

We allow for a human driver to temporarily take control of their vehicle. This could include a driver performing an emergency brake, reducing speed, temporarily maintaining a large distance from the predecessor vehicle outside of the desired chosen headway, or a legacy vehicle. We make the minimum assumption that the vehicle and driver will obey performance limits of their vehicle and road rules. Thus, constraints C3–6 apply to a human driver.

A. Formal Problem Statement

We now summarize the platoon control objective in a formal optimization framework. Given the platoon dynamics in (5), the augmented state $X_k \in \mathbb{R}^{3M}$ and control vector $U_k \in \mathbb{R}^M$, the goal is to steer the platoon towards the target velocity v_d and desired inter-vehicle distances $\bar{d}_k^{(i)}$ in (6), while respecting the safety and performance constraints C1–C6 for all vehicles $i = 1, \dots, M$ and all time steps.

At each time k, vehicle j has access only to a local information set $\mathcal{I}_k^{(j)}$, which collects its own sensor measurements and all successfully received packets from other vehicles. Based on $\mathcal{I}_k^{(j)}$, vehicle j constructs a local estimate of the platoon state,

$$\hat{X}_k^{(j)} = \mathbb{E}[X_k | \mathcal{I}_k^{(j)}],$$

with the distributed estimation. Using $\hat{X}_k^{(j)}$ as initial condition, vehicle j then solves a finite-horizon optimal control problem over a prediction horizon of length N. Let

$$\Delta U_k \triangleq \begin{bmatrix} \Delta U_{k|k}^\top & \Delta U_{k+1|k}^\top & \cdots & \Delta U_{k+N-1|k}^\top \end{bmatrix}^\top$$

be the stacked vector of predicted control vector, where $\Delta U_{k+\ell|k} = [\Delta u_{k+\ell|k}^{(1)}, \dots, \Delta u_{k+\ell|k}^{(M)}]^\top$ denotes the change in control for all vehicles at prediction step $\ell = 0, \dots, N-1$. For vehicles temporarily under human control, the corresponding entries are replaced by the predicted human action sequence $\Delta \hat{U}_k^{(\ell)}$. The predicted platoon state trajectory $\{X_{k+\ell|k}\}_{\ell=0}^N$ is generated according to

$$\begin{aligned} X_{k|k} &= \hat{X}_k^{(j)}, \\ X_{k+\ell+1|k} &= A_M X_{k+\ell|k} + B_M U_{k+\ell|k}, \quad \ell = 0, \dots, N-1, \end{aligned}$$

with

$$U_{k+\ell|k} = U_{k-1} + \sum_{r=0}^{\ell} \left(\alpha_{k+r}\Delta U_{k+r|k} + \bar{\alpha}_{k+r}\Delta\hat{U}_{k+r|k}\right).$$

Then, the decentralized platoon control problem at time k and vehicle j can then be formally stated as

$$\begin{aligned} \min_{\Delta U_k} \quad & J\big(\hat{X}_k^{(j)}, \Delta U_k\big) \\ \text{s.t.} \quad & X_{k+\ell+1|k} = A_M X_{k+\ell|k} + B_M U_{k+\ell|k}, \\ & \qquad \ell = 0, \dots, N-1, \\ & \text{constraints C1–C6 hold for all } i = 1, \dots, M, \\ & \qquad \text{and all prediction steps } \ell = 0, \dots, N, \\ & \Delta U_k \in \mathcal{U}, \quad X_{k+\ell|k} \in \mathcal{X}, \\ & U_{k+\ell|k} \text{ respects actuator bounds and rate limits,} \\ & X_{k|k} = \hat{X}_k^{(j)}, \end{aligned} \tag{7}$$

where $J(\cdot,\cdot)$ is a finite-horizon cost function that penalizes deviations from the target velocity v_d, desired inter-vehicle distances $\bar{d}_k^{(i)}$, and excessive control actions. The explicit quadratic structure of $J(\cdot,\cdot)$ and its implementation as a quadratic program are detailed in Section V-B (see in particular (11)–(12)).

Once (7) is solved, only the component corresponding to vehicle j, i.e., $\Delta u_{k|k}^{(j)}$, is applied to the physical vehicle, while the remaining components of $\Delta U_{k|k}$ are treated as virtual control variables. At the next time step, the information set $\mathcal{I}_{k+1}^{(j)}$ is updated based on new sensor and communication data, the estimator produces a new state estimate $\hat{X}_{k+1}^{(j)}$, and the optimization problem (7) is solved again in a receding horizon.

In a practical implementation, due to the sensors available on each vehicle, only a subset of the vehicle states are measured. Additionally, the control action would be individually computed at each vehicle. Our problem is to distribute the state estimation and control action computation to be local at each vehicle.

First, the desire to keep the full platoon together necessitates a control design which utilizes state information from all vehicles in the platoon. The control design needs to achieve convergence to both the desired velocity and time-varying inter-vehicle distances, while also ensuring the system and safety constraints C1–6. To accommodate temporary interruption from a human-driver requires the control design to react to the current state of the platoon. Second, due to the beaconing-based communication, the measurement sampling at each vehicle in the platoon is an offset within the sampling window. To enable combination of the measurements sampled at different offset times, we developed our multi-rate sampling process presented in Section IV-B. Third, the platoon control requires full platoon state information but each vehicle only measures a subset of the platoon. It is necessary to combine the received measurements to compute an estimate of the full platoon state for the control algorithm. We present a measurement fusion approach in Section IV-C.

IV. Platoon State Estimation

State estimation under communication constraints has been extensively studied in the context of networked systems.

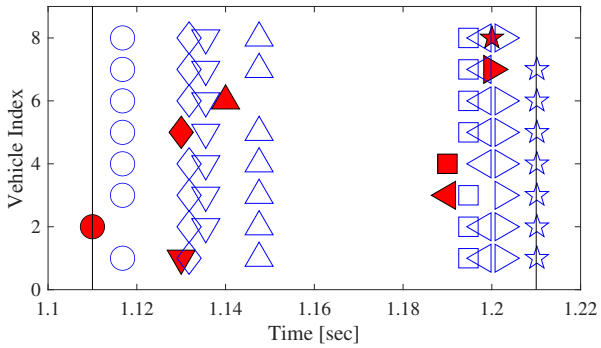

Figure 3. Plexe Experiment: packet transmission schedule and receipt delays. Sampling window is denoted with vertical black lines. Poor choice of window leads to receipts in the next window. Open symbol indicates packet receipt in the line of the vehicle received. Colored red packet is transmission time. Symbol indicates vehicle index: upside down triangle, circle, left-triangle, square, diamond, triangle, right-triangle, star, from vehicle 1 to-8, respectively.

For instance, [44] investigates state estimation for recurrent neural networks under stochastic intermittent transmission, which provides valuable insights into handling communication-induced uncertainties in distributed estimation problems. In this section, we will develop a distributed platoon state estimation framework combining the local measurements at each vehicle and the beaconing-based communication between vehicles. We seek to form a state estimate $\hat{X}_k^{(i)}$ at each vehicle to enable the decentralized computation of the control action at every vehicle i. We start by introducing a multi-rate dynamical model. Utilizing the multi-rate dynamics with intermittent sampling, we pose a measurement fusion algorithm to combine the received measurements from each vehicle. Finally, we summarize our decentralized estimation and control strategy.

A. Sampling Window Choice

In beaconing-based communication using CSMA/CA-based channel access, the transmissions from each vehicle are scheduled so as not to interfere with other vehicles. Each vehicle transmits at intervals defined by a sampling interval Δ_t. Regardless of the choice of the initial offset t_0, there will be at most one transmission from each vehicle within a given window between discrete indexes k and $k+1$. However, due to the inherent randomness of communication delays, it is possible to choose a window inappropriately, resulting in the packet being received in the subsequent sampling window instead of the intended one. This is visualized in Figure 3 with discrete-time indexes in vertical black lines.

To mitigate this, the temporal placement of scheduled transmissions and the typical maximum packet delay must be carefully considered. By selecting an appropriate initial offset t_0, packets can typically be received within the intended sampling window. Through careful analysis, an appropriate window is shown in Figure 2. This allows for packets to be received within the sampling period Δ_t, thereby ensuring that the control computation has enough time to process all received packets within this period.

B. Multi-Rate Sampling

Under the inter-vehicle communication, the measurement samples are delayed from the discrete-time index k, regardless

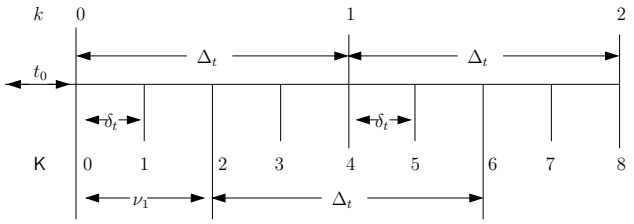

Figure 4. Visualization of the multi-rate process for $S = 4$. The control actions occur with large sampling rate Δ_t with discrete-time index k (top). There is a faster sampling of the process with smaller rate δ_t at discrete-time index K (middle). Every vehicle i measures and transmit with the sampling rate Δ_t with a fixed delay ν_i. As an example, vehicle 1 has a delay of $\nu_1 = 2$ samples (bottom).

of the choice of sampling window. As shown in Figure 2, the measurements are sampled at different offset times. The challenge arises in how to incorporate these measurement samples from different offset times to generate a platoon state estimate, thereby designing the decentralized platoon controller. In the following, we will develop a multi-rate sampling mechanism to address this issue.

Consider a new fast sampling rate δ_t [s/sample] where $\delta_t < \Delta_t$. We choose δ_t as a fraction of the actual sampling rate Δ_t such that $S = \Delta_t/\delta_t$ is an integer number of *fast* samples per slow sampling period, see Figure 4. Utilizing the window choice in Section IV-A, each vehicle then samples once every S *fast* samples. From each discrete-time index k, every vehicle i samples with a fixed time delay δ_i [s] which corresponds to a step delay of ν_i [samples] such that $\delta_i = \nu_i\delta_t$ where $0 \leq \nu_i < S$. A given vehicle i, will sample at times $t = k\Delta_t + \nu_i\delta_t + t_0$ for $k > 0$. Let us define K as a second fast discrete-time index and initialized such that both indexes start at the same time $k = \mathsf{K} = 0$. The discrete-time index k is the index for the control algorithm and uses the sampling rate Δ_t. This same sampling rate is used in the measurement sampling and communication technology. The relation between the control step k and sampling step K is $t = k\Delta_t = \mathsf{K}\delta_t$ and is visualized in Figure 4.

The platoon dynamics in Equation (3) can be discretized at the new sampling rate δ_t

$$X_{\mathsf{K}+1} = A_{M,\delta}X_{\mathsf{K}} + B_{M,\delta}U_{\mathsf{K}} + W_{\mathsf{K}} \tag{8}$$

where $A_{M,\delta}$ and $B_{M,\delta}$ are block diagonal matrices of the collection of single-vehicle dynamics and control input matrices at sampling rate δ_t, W_{K} is a vector of the i.i.d. process noise which is modeled as $W_{\mathsf{K}} \sim \mathcal{N}(0, \mathcal{W}_\delta)$, and X_{K} and U_{K} have the same definition as Equation (2) at time step K. The discretized matrices $A_{M,\delta}$ and $B_{M,\delta}$ can be computed as shown in [35] by replacing Δ_t with δ_t utilizing the method in [45]. The process noise covariance $\mathcal{W}_\delta$ is related to $\mathcal{W}$ in Equation (3) by $\mathcal{W}_\delta = \mathcal{W}\delta_t/\Delta_t$.

We consider that the control action U_{K} is held constant across the sampling window from K to $\mathsf{K} + S$ where $\mathsf{K} = k\Delta_t/\delta_t$ and $\mathsf{K} + S = (k+1)\Delta_t/\delta_t$. The sequence of process noises W_{K} in the interval each with covariance of $\mathcal{W}_\delta$, has the same covariance of $\mathcal{W}$. It can be shown that for a given $X_{\mathsf{K}} = X_k$ and constant control action over the window, we have $X_{\mathsf{K}+S} = X_{k+1}$.

The measurement of a vehicle i that occurs at sample K is

$$y_{\mathsf{K}}^{(i)} = \bar{\gamma}_{\mathsf{K}}^{(i)}(C_i X_{\mathsf{K}} + \mathfrak{v}_{\mathsf{K}}^{(i)}) \tag{9}$$

where the indicator $\bar{\gamma}_{\mathsf{K}}^{(i)} = 1$ at $\mathsf{K} = kS + \nu_i$ for $k > 0$, otherwise $\bar{\gamma}_{\mathsf{K}}^{(i)} = 0$. Note that as each vehicle is sampled with rate Δ_t, the measurement noise covariance defined in Section II-D is the same, there is just the time offset.

C. Measurement Fusion

By utilizing the multi-rate sampling mechanism, we establish new system dynamics as described by (8) and (9). The problem remains to combine the temporally offset and intermittently received measurements into a useful state estimate to compute the decentralized control actions. We now present a method to produce an estimate of the platoon state X_k at every vehicle. For a vehicle j, we define the state estimate as the expectation of the state given the information: $\hat{X}_k^{(j)} = E[X_k|\mathcal{I}_k^{(j)}]$ where $\mathcal{I}_k^{(j)}$ is the information set available at the vehicle j at time k. Each transmitted packet contains the following information:

- vehicle identifier – index i,
- measurement sampling index $\mathsf{K} = (k-1)S + \nu_i$,
- measurement $y_{\mathsf{K}}^{(i)}$,
- last implemented control action $u_{k-1}^{(i)}$, and
- identifier if the vehicle is under human-driver control.

If a packet is received within the control system sampling window Δ_t (i.e., the measurement sampled at time $\mathsf{K} = (k-1)S+\nu_i$ and received before time $\mathsf{K} = kS$), then it is considered a successful receipt; otherwise, we consider that the packet is dropped. Let us define $\gamma_{\mathsf{K}}^{(i,j)}$ as indicator that a packet transmitted at time K from vehicle i is received by vehicle j

$$\gamma_{\mathsf{K}}^{(i,j)} = \begin{cases} 1, \text{packet is received from vehicle } i \text{ at vehicle } j \\ 0, \text{otherwise.} \end{cases}$$

for all vehicle $i, j = 1, \ldots, M$. We define $\gamma_{\mathsf{K}}^{(i,i)} = 1$ as the local measurements at vehicle i are always available. In case of no transmission at time K, we define $\gamma_{\mathsf{K}}^{(i,0)} = 0$.

The information set $\mathcal{I}_k^{(j)}$ contains packet receipt outcomes, and successfully received packets from all platoon vehicles

$$\mathcal{I}_k^{(j)} = \{\gamma_{(\mathsf{k}-1)\mathsf{S}+\nu_1}^{(1,j)}, \gamma_{(\mathsf{k}-1)\mathsf{S}+\nu_1}^{(1,j)} y_{\gamma_{(\mathsf{k}-1)\mathsf{S}+\nu_1}}^{(1)}, \ldots, \gamma_{(\mathsf{k}-1)\mathsf{S}+\nu_\mathsf{M}}^{(M,j)}, \gamma_{(\mathsf{k}-1)\mathsf{S}+\nu_\mathsf{M}}^{(M,j)} y_{\gamma_{(\mathsf{k}-1)\mathsf{S}+\nu_\mathsf{M}}}^{(M)}\} \cup \mathcal{I}_{k-1}^{(j)}$$

for $j = 1, \ldots, M$, where the initial information is the empty set $\mathcal{I}_0^{(j)} = \varnothing$.

Due to effects in the communication channel, all transmitted packets will be received with random delay. The Plexe experiment (see Section II-E) motivates the following estimation procedure. Through appropriate choice of the sampling window (see Section IV-A and Figure 2), all packets will be received well before the next control action sampling time k. However, as noted in Section II-E, packets may be dropped due to bit errors, interference, or low SNR during transmission. Considering the existence of packet dropouts, we choose a maximum permitted receipt delay δ_D from the last vehicle to be sampled. After this maximum delay, all packets have either been successfully received or are considered dropped.

At time $\mathsf{K} = (k-1)S + \max_i \nu_i + \delta_D$ we can predict a state estimate at time k as there will be no further packets after $\mathsf{K} = (k-1)S + \max_i \nu_i + \delta_D$. First, we update $\bar{U}_{k-1}^{(j)}$ using known control actions, or use the previous locally computed control action. Second, towards the end of the slower sampling period we batch process the successfully received measurements from time $\mathsf{K} = (k-1)S$ to $\mathsf{K} = (k-1)S + \max_i \nu_i$. We design δ_D to leave time for the computation of the control actions. Third, we predict the state forward from time $\mathsf{K} = (k-1)S + \max_i \nu_i$ to the next control action time $\mathsf{K} = kS$. Finally, we compute the optimal change in control action using the platoon state estimate $\hat{X}_{kS}$, updated previous control action $\bar{U}_{k-1}^{(j)}$ and human-driver identifier.

To combine the intermittent measurements, and to produce a state estimate, we can utilize the Kalman filter with intermittent observations [46] with a time-varying and random measurement matrix [47]. In batch processing the filter, every measurement taken at time K is available exactly when obtained, i.e., at time K. The state estimate at time K for $\mathsf{K} < kS$ is $\hat{X}_{\mathsf{K}}^{(j)} = E[X_{\mathsf{K}} | \mathcal{I}_k^{(j)}]$. The state estimates then follow the following equations:

$$
\begin{aligned}
\hat{X}_{\mathsf{K}}^{(j)} &= (I - K_{\mathsf{K}}^{(j)} C_{j,\mathsf{K}})(A_{M,\delta} \hat{X}_{\mathsf{K}-1}^{(j)} + B_{M,\delta} \bar{U}_{k-1}^{(j)}) + K_{\mathsf{K}}^{(j)} z_{\mathsf{K}}^{(j)} \\
P_{\mathsf{K}}^{(j)} &= (I - K_{\mathsf{K}}^{(j)} C_{j,\mathsf{K}})(A_{M,\delta} P_{\mathsf{K}-1}^{(j)} A_{M,\delta}^{\mathsf{T}} + \mathcal{W}_\delta) \\
K_{\mathsf{K}}^{(j)} &= (A_{M,\delta} P_{\mathsf{K}-1}^{(j)} A_{M,\delta}^{\mathsf{T}} + \mathcal{W}_\delta) C_{j,\mathsf{K}}^{\mathsf{T}} \\
&\quad (C_{j,\mathsf{K}} (A_{M,\delta} P_{\mathsf{K}-1}^{(j)} A_{M,\delta}^{\mathsf{T}} + \mathcal{W}_\delta) C_{j,\mathsf{K}}^{\mathsf{T}} + \mathcal{R}_i)^{-1} \qquad (10)
\end{aligned}
$$

where $\bar{U}_{k-1}^{(j)}$ is the control action to the platoon. $z_{\mathsf{K}}^{(j)}$ represents the full set of measurements received between time $\mathsf{K}-1$ to K. $K_{\mathsf{K}}^{(j)}$ is the Kalman filter gain matrix. Specifically, if a packet is successfully received from transmitting vehicle i ($i = 1, \ldots, M$) at time K, indicated by $\gamma_{\mathsf{K}}^{(i,j)} = 1$, then $z_{\mathsf{K}}^{(j)} = [\ldots, (y_{\mathsf{K}}^{(i)})^{\mathsf{T}}, \ldots]^{\mathsf{T}}$. Here $\tilde{\mathsf{K}}$ denotes a time index before K. If no packet is received, the corresponding elements in $z_{\mathsf{K}}^{(j)}$ are set to 0.

We denote the control action based on the information available to vehicle j at time $k-1$ as $\bar{U}_{k-1}^{(j)}$. In the situation that a packet is successfully received, we set the ith element of $\bar{U}_{k-1}^{(j)}$ as $u_{k-1}^{(i)}$ and utilize the known applied control action from vehicle i. In the case of a dropout from vehicle i we use the ith output from the locally computed control action, which was computed based on the best information available about the platoon $\bar{U}_{k-2}^{(j)} + \Delta\hat{U}_{k-1}^{(j)}$. We note that the proposed framework does not require guaranteed full-state exchange nor permanent all-to-all communication. Instead, vehicles operate under partial, asynchronous, and lossy information exchange.

V. Decentralized Platoon Control Design

Based on the distributed platoon state estimation, each vehicle now has its own platoon state estimate. In this section, we present a practical implementation of decentralized MPC that utilizes these individual platoon state estimates. Unlike traditional decentralized control—where each vehicle computes only its own control action—our approach enables each vehicle to compute an augmented control vector for the entire platoon while applying only the portion relevant to itself. Controllers are embedded within each vehicle and rely solely on local information from the vehicle itself and its neighbors. Thus, while our method differs from traditional decentralized control, it remains decentralized in nature. This approach smoothly controls the platoon to the desired inter-vehicle distances and platoon velocity while ensuring constraints C1–6. Additionally, the design also incorporates a human driver temporarily taking control of their vehicle.

A. Human Driver Prediction Model

MPC optimizes the change in control actions over a finite horizon of N time steps into the future. Ideally for the platoon controller, future human driver control actions $\Delta\mathcal{U}_k$ are known exactly. This motivates the need to predict the potential control action for the human driver. For a finite prediction horizon of length N, the predicted state of the human-driver vehicle ℓ can be written as a function of the current state and a sequence of predicted control actions $\Delta\hat{\mathcal{U}}_k^{(\ell)} = [\Delta\hat{\mathrm{u}}_{k+1|k}^{(\ell)}, \ldots, \Delta\hat{\mathrm{u}}_{k+N-1|k}^{(\ell)}]^{\mathsf{T}}$. To predict the future control inputs of the human-driven vehicle, we assume that the human driver maintains a constant control input over the finite MPC prediction horizon, unless constrained by physical or legal bounds. This simplification allows tractable prediction and is commonly used in hybrid human–autonomy systems [13]. However, we acknowledge that human drivers are often more variable and reactive than autonomous agents, particularly during sudden braking or emergency maneuvers [48]. Therefore, the constant-input assumption only serves as a baseline model.

The above motivates us to consider a quadratic cost function that only penalizes changes in control

$$
\bar{J}(\hat{X}_{kS}^{(\ell)}, \Delta\hat{\mathcal{U}}_k^{(\ell)}) = \sum_{j=0}^{N-1} (\Delta\hat{\mathcal{U}}_{k+j|k}^{(\ell)})^{\mathsf{T}} r_\Delta (\Delta\hat{\mathcal{U}}_{k+j|k}^{(\ell)}) \qquad (11)
$$

where r_Δ is the ℓth diagonal element of R_Δ. In the absence of constraints, this cost function is minimized when $\Delta\hat{\mathcal{U}}_k^{(\ell)} = 0$. However, as mentioned in the preceding section, we assume the human driver obeys the constraints on velocity and acceleration C3–6. Over the prediction horizon, the corresponding state constraints can be written as a linear matrix inequality of the vector of predicted change in control actions $\Delta\hat{\mathcal{U}}_k^{(\ell)}$, see [35]. The quadratic cost function in (11) with constraints can be minimized using standard quadratic programming solvers to find the minimum control action that meets the constraints. This constrained prediction of the human controlled vehicle ℓ control action, $\Delta\hat{\mathcal{U}}_k^{(\ell)}$, is utilized in the computation for the decentralized platoon control, as described below.

Remark 2. *For the human-driving behavior modeling beyond constant-input assumption, future extensions may incorporate data-driven driver-intent prediction methods, such as reinforcement learning or Gaussian process–based forecasting. Alternatively, we can model mixed-autonomy platoons as a switching system, where the controller transitions between autonomous control mode and human-operated mode whenever driver intervention occurs. This would allow the control strategy to explicitly account for changes in driving authority.*

B. Cost Function Design

Consider for each vehicle i for all $i = 1, \dots, M$, the absolute position, velocity, and acceleration errors as the difference between the current state and desired reference $\xi_k^{(i)} = p_k^{(i)} - p_k^{(i)\star}$, $\zeta_k^{(i)} = v_k^{(i)} - v_k^{\star}$, and $\psi_k^{(i)} = a_k^{(i)} - a_k^{\star}$. For the entire platoon, these errors can be written as $X_k - X_k^{\star} = [\xi_k^{(1)}, \dots, \xi_k^{(M)}, \zeta_k^{(1)}, \dots, \zeta_k^{(M)}, \psi_k^{(1)}, \dots, \psi_k^{(M)}]$. For convenience, we define $\hat{\eta}_{k+j|k}^{(i)}$, $\hat{\xi}_{k+j|k}^{(i)}$, $\hat{\zeta}_{k+j|k}^{(i)}$, and $\hat{\psi}_{k+j|k}^{(i)}$ as the predicted errors where the subscript indicates the state prediction at time $k+j$ given the state at time k.

Following [36] and [37], we introduce virtual reference vehicles on the platoon boundary that perfectly follow the reference $p_k^{(0)} = p_k^{\star}$, $p_k^{(M+1)} = p_k^{(M+1)\star}$, $v_k^{(0)} = v_k^{(M+1)} = v_k^{\star}$, and $a_k^{(0)} = a_k^{(M+1)} = a_k^{\star}$, and introduce the relative position error between vehicle i and vehicle $(i-1)$ for all $i = 1, \dots, M$ as $\eta_k^{(i)} = p_k^{(i)} - p_k^{(i-1)} + \bar{d}_k^{(i)}$. Based on the MPC design, we define the predicted value of the change in control as

$$\Delta \hat{U}_k \triangleq [\Delta \hat{U}_{k|k}^T, \dots, \Delta \hat{U}_{k+N-1|k}^T]^T$$

where $\Delta \hat{U}_{k+j|k} = [\Delta u_{k+j|k}^{(1)}, \dots, \Delta u_{k+j|k}^{(M)}]$ with $j = 0, \dots, N-1$.

Inspired by the infinite horizon cost function in [37], we propose a finite horizon cost function over a prediction horizon of N steps with our time-varying references

$$\begin{aligned} J = \sum_{j=0}^{N-1} \Bigg[\sum_{i=1}^{M+1} q_1 \left(\hat{\eta}_{k+j|k}^{(i)}\right)^2 + \sum_{i=1}^{M} \Bigg(q_2 \left(\hat{\xi}_{k+j|k}^{(i)}\right)^2 \\ + q_3 \left(\hat{\zeta}_{k+j|k}^{(i)}\right)^2 + q_4 \left(\hat{\psi}_{k+j|k}^{(i)}\right)^2 + r \left(\Delta u_{k+j|k}^{(i)}\right)^2 \Bigg) \Bigg] \\ + (\hat{X}_{k+N|k} - X_{k+N}^{\star})^{\mathsf{T}} P_{k+N} (\hat{X}_{k+N|k} - X_{k+N}^{\star}) \end{aligned} \quad (12)$$

where q_1 is the penalty on relative position error, q_2 the penalty on absolute position error, q_3 the penalty on velocity error, q_4 as the penalty on the acceleration, r the penalty on the control inputs, and P_{k+N} is the terminal state cost. To achieve convergence independent of platoon length, it is necessary to penalize both the relative and the absolute position errors [37]. The state $\hat{X}_{k+j|k}$ can be computed using the dynamics Equation (5) and the predicted human-driver action $\Delta \hat{\mathcal{U}}_k$.

Using algebraic manipulation and Equation (6), the relative position error $\eta_k^{(i)}$, can be written as a function of the errors $\eta_k^{(i)} = \xi_k^{(i)} - \xi_k^{(i-1)} + h_k^{(i)} \zeta_k^{(i)}$ such that the relative position errors can be incorporated as cross-terms of the absolute position errors and velocity errors, with the headway times as a weight on the velocity errors. Although headway times could be interpreted as a reference to the problem introduced by the desired inter-vehicle distance (6), it is more practical to treat them as weights on state deviations.

Our cost function in Equation (12) can be efficiently written as a quadratic function of the platoon state estimate $\hat{X}_{kS+j|kS}^{(i)}$ and reference $X_{k+j}^{\star}$ for each vehicle i. Utilizing the platoon dynamics Equation (3) and writing the control in terms of changes in control action with the human driver Equation (4), our cost function can be written in the form of a quadratic program of the predicted control actions, i.e., $J(\hat{X}_{kS}^{(i)}, \Delta \hat{U}_k)$.

Algorithm 1 Decentralized Model Predictive Platoon Control

Inputs: Number of vechicles M, Mechanical actuation lags τ_i, Headway times $h_k^{(i)}$, Desired standstill distance r_i, Target velocity v_d, Constraints $\{d_{\min}, d_{\max}, v_{\min}, v_{\max}, a_{\min}, a_{\max}\}$, Number of fast samples S, Measurement sampling delay ν_i, Maximum permitted receipt delay δ_D, Reference sampling periods k_m, Prediction horizon N, Cost function weights $\{q_1, q_2, q_3, q_4, r\}$, the scheduled time interval Δ_t and the time offset t_0.
for time steps $k = 0, 1, \dots$ **do**
  Compute the platoon state estimate $\hat{X}_{kS}^{(i)}$ for each vehicle i using (10).
  if a vehicle is under human driver control **then**
    Determine the vehicle ℓ controlled by human driver
    Reset state reference based on ℓ position and velocity [35, Section V-A]
    Predict the potential control action for the human driver $\Delta \hat{\mathcal{U}}_k^{(\ell)}$ by minimizing (11) subject to constraints C1-6
  end if
  Compute state reference [35, Section V-A]
  Compute the optimal change in control action $\Delta \hat{U}_k^{\star}$ in (13) for each vehicle subject to constraints C1-6
  Implement latest control action $\Delta u_{k|k}^{(i)}$ on the vehicle $i = 1, \dots, M$
  Step platoon dynamics
end for

Over the prediction horizon, the state constraints C1–6 can be written as a linear matrix inequality of the vector of predicted change in control actions $\Delta \hat{U}_k$, see [35].

The optimal platoon control action is the change in control that minimizes the constrained finite horizon cost function

$$\Delta \hat{U}_k^{\star} = \min_{\Delta \hat{U}_k} J(\hat{X}_{kS}^{(i)}, \Delta \hat{U}_k). \quad (13)$$

Following the rolling horizon approach only the first element $\Delta u_{k|k}^{(i)}$ is implemented on the vehicle i. Each vehicle conducts the optimization (13) based on its own platoon state estimate and adopts the corresponding control action. At the next time step, the optimization is recomputed on the new state information. The implementation of decentralized platoon control is summarized in Algorithm 1.

C. Theoretical Properties

While the proposed framework is primarily developed for practical deployment, it is also important to examine whether the decentralized control framework preserves desirable analytical properties such as feasibility, boundedness of estimation error, and closed-loop stability. The goal of this subsection is not to provide a full theoretical derivation, but rather to establish analytical grounding and demonstrate that the proposed structure is consistent with existing results in decentralized MPC and state estimation under intermittent communication. We begin by formalizing the modeling assumptions relevant to the theoretical analysis.

Assumption 1. *(Packet Loss Model) The communication channels among vehicles follow an independent Bernoulli packet-loss process with packet arrival probability $\mu > 0$.*

Assumption 2. *(Bounded Human Override) The human override inputs satisfy $\|\Delta \mathbf{u}_k^{(i)}\| \leq \varepsilon$, where $\varepsilon \geq 0$ depends on physical and regulatory limits.*

Assumption 3. *(Convex MPC Formulation) The cost function in the decentralized optimization problem is convex with polyhedral constraints, and there exists a terminal set ensuring recursive feasibility.*

These assumptions allow us to explore whether the controller remains feasible under communication uncertainties and whether the estimation error remains bounded, which are necessary conditions for closed-loop stability.

Theorem 1. *(Recursive Feasibility) Consider the decentralized MPC problem under Assumptions 1–3. If the optimization problem is feasible at $k = 0$, then feasibility is preserved for all $k \geq 0$ with probability at least μ^M, where M is the platoon size.*

Proof. Since the optimization problem is convex with a compact feasible set at initialization, recursive feasibility follows from established robust MPC results. The bounded estimator uncertainty implied by Theorem 2 ensures that future state trajectories remain within a constraint-invariant tube. With bounded human override inputs, feasibility is preserved using standard arguments from robust tube-based MPC [49], [50]. The probabilistic factor arises from intermittent communication affecting estimator refresh rates. □

Intuitively, Theorem 1 guarantees that the controller will not fail because of temporary packet losses or isolated aggressive human interventions, as long as these effects remain within the modeled bounds.

Theorem 2. *(Bounded Estimation Error) Under Assumption 1, the estimator in Section IV satisfies*

$$\limsup_{k\to\infty} \mathbb{E}\|X_k^{(j)} - \hat{X}_k^{(j)}\|^2 \leq \frac{C}{1-\mu},$$

for some finite constant $C > 0$ depending on noise covariances and platoon dynamics.

Proof. The estimator follows the structure of a Kalman filter with intermittent observations. From [46], [51], mean-square boundedness holds when μ exceeds a critical connectivity threshold. The multi-rate sampling mechanism introduced in Section IV does not alter the stochastic observability structure, and thus the stability result directly applies. □

This result indicates that although packet drops influence estimation accuracy, the effect remains bounded and does not diverge over time, provided communication quality is above the threshold derived in prior literature.

Corollary 1. *If Theorems 1 and 2 hold, then the closed-loop platoon system is input-to-state practically stable with respect to packet dropouts and bounded human override inputs.*

Table II
SIMULATION PARAMETERS FOR PLATOON MOBILITY

Parameter	Value
Car Following (CF) model	ACC and CACC
Driving speed	100 km/h
Max acceleration	2.5 m/s^2
Max deceleration	9.0 m/s^2
Driver imperfection σ	0.5
Driver's desired minimum headway τ	0.5 s
ACC headway T	1.2 s
CACC constant spacing d_d	5 m
CACC bandwidth ω_n	0.2 Hz
CACC damping ratio ξ	1
CACC weighting factor C_1	0.5
Simulation time	120 s
Random seeds	10 repetitions

This corollary implies that the decentralized platoon can tolerate real-world uncertainties and still converge toward the desired formation and velocity. While degradation may occur under severe communication constraints or highly variable human interventions, the underlying controller remains stable.

Remark 3. *A full formal stability proof under mixed human participation and large-scale networked communication is beyond the scope of this implementation-focused study. However, the above theoretical results demonstrate that the proposed decentralized MPC inherits feasibility and practical stability guarantees from established decentralized MPC and intermittent estimation theory. Extending these guarantees to general communication topologies and large platoon formations will be addressed in future work.*

VI. EVALUATION

In this section, we will explore the performance of the decentralized platoon control design with some simulation examples. We first perform a numerical experiment using the packet receipt outcomes from a Plexe experiment. We then further explore the performance in a Monte Carlo simulation with randomized packet receipt outcomes.

A. Decentralized Control Action

For our numerical experiment, we consider again the scenario from Section II-E. The scheduling time interval is set to $\Delta_t = 0.1$ [s/sample]. Following Section IV-A, we select the initial time offset as $t_0 = 1.18$ [s] to achieve the window shown in Figure 2. Following Section IV-A, we select the fast sampling rate as $\delta_t = 0.1$ [s/sample] and $S = 10$. Following Section IV-C, we select the maximum receipt delay as 0.0108 [s]. For every successfully received message, we measure a collection of metrics at the corresponding receiving vehicles. Further details of our simulation setup are listed in Tables I and II. A sample of the packet receipt outcomes is visualized in Figure 2.

For comparison with centralized approach, we revisit the numerical experiment in [35], where the desired inter-vehicle distances are $d_2 = 8.5$, $d_3 = 7.5$, $d_4 = 10.5$, $d_5 = 9.5$, $d_6 = 11.5$, $d_7 = 9.5$, $d_8 = 10.5$ and constant time headways are $h_2 = 1.3$, $h_3 = 1.5$, $h_4 = 0.8$, $h_5 = 1.2$, $h_6 = 1.1$,

$h_7 = 0.9$, and $h_8 = 0.94$ [s]. vehicle 3 performs an emergency brake at time 100 [sec], before briefly traveling at a lower velocity of 11 [m/s] at 150 [s]. At time 250 [sec] vehicle 3 returns to the platoon. At time 350 [sec] the vehicles all increase their constant time headways to $h_2 = 3$, $h_3 = 2.6$, $h_4 = 4$, $h_5 = 2.5$, $h_6 = 2$, $h_7 = 2.1$, and $h_8 = 1.8$ [s]. Figure 5 shows the inter-vehicle distances, and Figure 6 illustrates the vehicle velocities using the proposed decentralized control strategy. It can be found that the performance of the centralized platoon controller operated in a decentralized wireless manner remains very high. Minimal performance differences can be seen to the five-vehicle platoon example in [35].

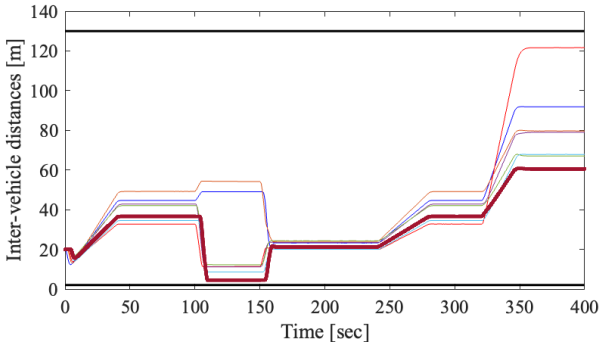

Figure 5. Inter-vehicle distances between the $M = 8$ vehicles from the Plexe experiment. Measurements are shared via inter-vehicle communications. Vehicles converge to the desired inter-vehicle distance following the reference. vehicle 3 performs an emergency brake, at time 100 [s], then starts driving at 11 [m/s] at 150 [s], finally returning to the platoon at time 250 [s]. At time 350 [s] all drivers select a new time headway.

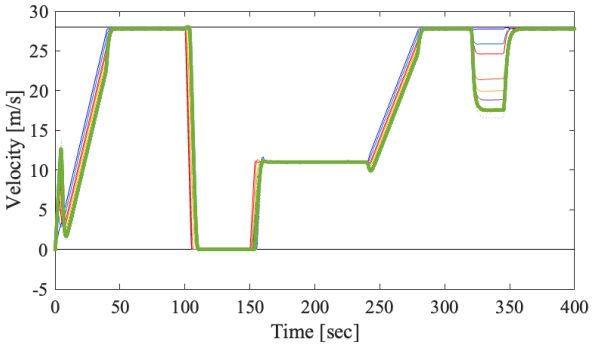

Figure 6. Velocities of the $M = 8$ vehicles from the Plexe experiment. Measurements are shared via inter-vehicle communications.

B. Impact of Channel Quality

In our current work, we conducted simulation of realistic inter-vehicle communication using the Plexe platform, which incorporates detailed DSRC (IEEE 802.11p)-based communication with random channel access delays, packet drops, and interference. Specifically, our framework includes a multi-rate measurement fusion mechanism and a maximum delay threshold to model asynchronous packet receipt and losses effectively. This allows us to capture essential properties of non-uniform sampling and communication unreliability even within the simulation environment. Following the high quality performance of our proposed decentralized design from the Plexe experiment data, we explore the performance of our controller across a range of channel qualities in a Monte Carlo study of 1000 trials at each channel quality. In our simulation we use a platoon of five vehicles, where vehicle 3 is taken over by the human driver, mirroring the experiment documented in [35].

To randomize the packet receipt outcomes, we redefine $\gamma_{\mathsf{K}}^{(i,j)} \in \{0,1\}$ as an i.i.d. Bernoulli random variable where $\mathsf{K} = (k-1)S + \nu_i$ for $k > 0$ as the time that vehicle i samples, for all vehicles-i, j for all $i, j = 1, \ldots, M$ and $i \neq j$. A successful receipt $\gamma_{\mathsf{K}}^{(i,j)} = 1$ under this network model means that a transmitted packet is successfully decoded at the receiver, and available before the maximum receipt delay. Thus, our model includes both packet drops and transmission delays.

We define $\mu_{i,j}$ as the (fixed) probability that a packet from vehicle i is successfully received by vehicle j[1]

$$\mu_{i,j} = \mathbb{P}(\gamma_{\mathsf{K}}^{(i,j)} = 1).$$

We recall that the model-predictive controller introduced in Section V minimizes a performance loss function over a rolling horizon, see (12) and (13). Accordingly, we will quantify the empirical performance of the controlled system through the stage cost in (12). To be more specific, the performance loss function $J_s(X_k, \Delta U_k)$ given below is evaluated on the empirical system states. This function quantifies deviations of the relative and absolute positions, velocities and accelerations from their desired values, as well as the applied control input

$$J_s(X_k, \Delta U_k) = \left[\sum_{i=1}^{M+1} q_1 \left(\eta_k^{(i)}\right)^2 + \sum_{i=1}^{M} \left(q_2 \left(\xi_k^{(i)}\right)^2 + q_3 \left(\hat{\zeta}_k^{(i)}\right)^2 + q_4 \left(\hat{\psi}_k^{(i)}\right)^2 + r \left(\Delta u_k^{(i)}\right)^2 \right) \right].$$

Figure 7 shows empirical averages of the stage cost against probability of successful packet receipt $\mu_{i,j}$. We observe that for lower quality channels the cost increases. This results from the lower quality state estimates due to the higher rate of unavailable packets. In particular, with more packets dropped, information about vehicle 3 when the human driver takes over and returns to the platoon, is temporally delayed. As such, the other vehicles in the platoon take larger control actions to more aggressively correct for the disturbance. Note that under perfect channel conditions (i.e., $\mu_{i,j} = 1$), the decentralized control strategy reduces to the centralized controller with a mean cost of approximately 2.35. As the packet reception probability decreases, the average cost of the decentralized strategy increases correspondingly. However, the performance degradation remains relatively modest-except in scenarios with extremely poor communication quality-indicating that the proposed decentralized controller maintains performance close to that of the ideal centralized controller. This result can

[1]Note that $\mu_{i,i} = 1$ as the measurements taken at vehicle i are always available to itself.

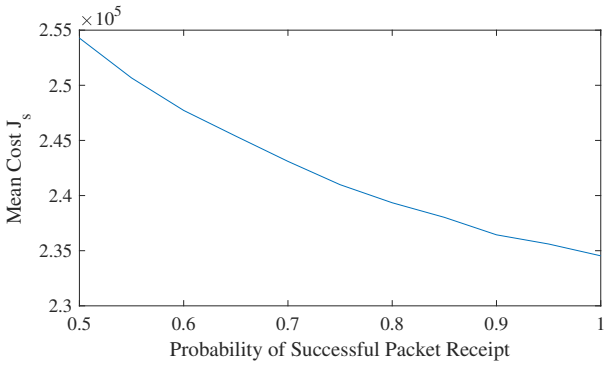

Figure 7. Performance loss $J_s(X_k, \Delta U_k)$ of the platoon against probability of packet receipt of the inter-vehicle communication, averaged over 1000 trials.

also serve as an implicit comparison between the decentralized and centralized control schemes.

For even lower quality channels, the lack of information for several control steps could, in extreme cases, result in vehicles violating constraints, e.g., inter-vehicle distances. In the case of substantially poor quality channels, this motivates the use of event based transmission policies [52]. With better channels, the quality of the centralised implementation is recovered.

The decentralized implementation of the proposed MPC and estimation framework is designed to be computationally tractable at the vehicle level. Each vehicle solves a local MPC problem with a fixed prediction horizon and a quadratic cost, subject to linear dynamics and constraints. This results in a per-step computational complexity of approximately $\mathcal{O}(N^3)$, where N is the horizon length. Due to the decentralized nature, the problem size does not scale with the total number of vehicles but only with the local model and constraint dimensions. For the state estimation component, each vehicle executes a recursive estimator that fuses asynchronous local and received measurements. The estimation update is linear in the state dimension and can be performed in real time, given the sparse communication structure. Our implementation indicates that both control and estimation cycles can be executed within tens of milliseconds on a standard processor, ensuring compatibility with typical vehicular control cycles (e.g., 100 ms).

Remark 4. *While our decentralized framework achieves near-centralized performance in small to medium-sized platoons*[2]*, scalability remains a challenge when the number of vehicles increases significantly. The requirement that each vehicle estimate the full platoon state can lead to high communication and computation overhead, particularly if some vehicles fall outside of others' communication range. To address this, future work may consider hierarchical platoon structures or partitioned estimation strategies, where each vehicle only maintains estimates for a limited set of neighbors based on communication availability or proximity [53]. Additionally, selective state abstraction techniques can be used to reduce the estimation dimensionality. These extensions would preserve local autonomy while ensuring scalability and robustness in large-scale platooning scenarios.*

[2]The term "medium-scale platoon" refers to formations of approximately 5–20 vehicles, consistent with current deployment models.

VII. Conclusion

This paper successfully demonstrates a novel decentralized MPC framework that effectively addresses the critical challenges of human-driver interaction in autonomous vehicle platooning. Through extensive Plexe simulations, we have shown that our proposed approach achieves performance comparable to centralized control systems while offering enhanced robustness to communication uncertainties and seamless accommodation of human driver interventions. The multi-rate measurement fusion strategy effectively handles asynchronous data sampling, while the distributed state estimation enables reliable platoon operation even under partial communication failures. The decentralized architecture not only reduces communication overhead but also improves scalability for larger platoons, making it well-suited for practical implementation.

Future work could explore the extension of this framework to handle more complex scenarios such as lane changes, merging maneuvers, and interaction with non-platooned vehicles. Incorporating driver behavior uncertainty or more expressive driver models into the decentralized controller is also an important direction for future work. Additionally, real-world testing and validation in a more sophisticated traffic flow scenario would provide valuable insights into the system's performance under varied environmental conditions and traffic patterns. A complete formal stability proof under dynamic participation of human-driven vehicles remains an open research direction.

References

[1] P. Zhu, S. Jin, X. Bu, and Z. Hou, "Distributed data-driven control for a connected autonomous vehicle platoon subjected to false data injection attacks," *IEEE Transactions on Automation Science and Engineering*, 2023.

[2] C. Sommer and F. Dressler, *Vehicular Networking*. Cambridge University Press, 2014.

[3] Y. Bian, C. Du, M. Hu, S. E. Li, H. Liu, and C. Li, "Fuel economy optimization for platooning vehicle swarms via distributed economic model predictive control," *IEEE Transactions on Automation Science and Engineering*, vol. 19, no. 4, pp. 2711–2723, 2021.

[4] S. Tsugawa, S. Jeschke, and S. E. Shladover, "A review of truck platooning projects for energy savings," *IEEE Transactions on Intelligent Vehicles*, vol. 1, no. 1, pp. 68–77, 2016.

[5] M. Azad, N. Hoseinzadeh, C. Brakewood, C. R. Cherry, and L. D. Han, "Fully autonomous buses: A literature review and future research directions," *Journal of Advanced Transportation*, vol. 2019, no. 1, p. 4 603 548, 2019.

[6] A. Alam, B. Besselink, V. Turri, J. Mårtensson, and K. H. Johansson, "Heavy-duty vehicle platooning for sustainable freight transportation: A cooperative method to enhance safety and efficiency," *IEEE Control Systems Magazine*, vol. 35, no. 6, pp. 34–56, 2015.

[7] B. Besselink, V. Turri, S. van de Hoef, K.-Y. Liang, A. Alam, J. Martensson, and K. H. Johansson, "Cyber–physical control of road freight transport," *Proceedings of the IEEE*, vol. 104, no. 5, pp. 1128–1141, May 2016.

[8] C. Wu, Z. Xu, Y. Liu, C. Fu, K. Li, and M. Hu, "Spacing policies for adaptive cruise control: A survey," *IEEE Access*, vol. 8, pp. 50 149–50 162, Mar. 2020.

[9] S. Feng, Y. Zhang, S. E. Li, Z. Cao, H. X. Liu, and L. Li, "String stability for vehicular platoon control: Definitions and analysis methods," *Annual Reviews in Control*, vol. 47, pp. 81–97, 2019.

[10] X. Xu, J. W. Grizzle, P. Tabuada, and A. D. Ames, "Correctness guarantees for the composition of lane keeping and adaptive cruise control," *IEEE Transactions on Automation Science and Engineering*, vol. 15, no. 3, pp. 1216–1229, 2017.

[11] D. Swaroop and J. K. Hedrick, "String stability of interconnected systems," *IEEE Transactions on Automatic Control*, vol. 41, no. 3, pp. 349–357, 1996.

[12] S. Santini, A. Salvi, A. S. Valente, A. Pescapé, M. Segata, and R. L. Cigno, "A consensus-based approach for platooning with intervehicular communications and its validation in realistic scenarios," *IEEE Transactions on Vehicular Technology*, vol. 66, no. 3, pp. 1985–1999, 2016.

[13] R. Yan, R. Jiang, B. Jia, J. Huang, and D. Yang, "Hybrid car-following strategy based on deep deterministic policy gradient and cooperative adaptive cruise control," *IEEE Transactions on Automation Science and Engineering*, vol. 19, no. 4, pp. 2816–2824, 2021.

[14] S. Zeadally, J. Guerrero, and J. Contreras, "A tutorial survey on vehicle-to-vehicle communications," *Telecommunication Systems*, vol. 73, no. 3, pp. 469–489, 2020.

[15] K. C. Dey, L. Yan, X. Wang, Y. Wang, H. Shen, M. Chowdhury, L. Yu, C. Qiu, and V. Soundararaj, "A review of communication, driver characteristics, and controls aspects of cooperative adaptive cruise control (CACC)," *IEEE Transactions on Intelligent Transportation Systems*, vol. 17, no. 2, pp. 491–509, 2015.

[16] C. Katrakazas, M. Quddus, W.-H. Chen, and L. Deka, "Real-time motion planning methods for autonomous on-road driving: State-of-the-art and future research directions," *Transportation Research Part C: Emerging Technologies*, vol. 60, pp. 416–442, 2015.

[17] F. Dressler, "Cyber physical social systems: Towards deeply integrated hybridized systems," in *2018 International Conference on Computing, Networking and Communications (ICNC)*, IEEE, 2018, pp. 420–424.

[18] J. Shi, Y. Gao, W. Wang, N. Yu, and P. A. Ioannou, "Operating electric vehicle fleet for ride-hailing services with reinforcement learning," *IEEE Transactions on Intelligent Transportation Systems*, vol. 21, no. 11, pp. 4822–4834, 2019.

[19] L. Sabattini, M. Aikio, P. Beinschob, M. Boehning, E. Cardarelli, V. Digani, A. Krengel, M. Magnani, S. Mandici, F. Oleari, et al., "The pan-robots project: Advanced automated guided vehicle systems for industrial logistics," *IEEE Robotics & Automation Magazine*, vol. 25, no. 1, pp. 55–64, 2017.

[20] J. A. Miller, S. Nikan, and M. H. Zaki, "Navigating the handover: Reviewing takeover requests in level 3 autonomous vehicles," *IEEE Open Journal of Vehicular Technology*, 2024.

[21] Z. Wang, G. Wu, and M. J. Barth, "A review on cooperative adaptive cruise control (CACC) systems: Architectures, controls, and applications," in *IEEE ITSC 2018*, IEEE, 2018, pp. 2884–2891.

[22] A. Talebpour and H. S. Mahmassani, "Influence of connected and autonomous vehicles on traffic flow stability and throughput," *Transportation research part C: emerging technologies*, vol. 71, pp. 143–163, 2016.

[23] F. Zheng, C. Liu, X. Liu, S. E. Jabari, and L. Lu, "Analyzing the impact of automated vehicles on uncertainty and stability of the mixed traffic flow," *Transportation research part C: emerging technologies*, vol. 112, pp. 203–219, 2020.

[24] W.-X. Zhu and H. M. Zhang, "Analysis of mixed traffic flow with human-driving and autonomous cars based on car-following model," *Physica A: Statistical Mechanics and its Applications*, vol. 496, pp. 274–285, 2018.

[25] W. Levine and M. Athans, "On the optimal error regulation of a string of moving vehicles," *IEEE Transactions on Automatic Control*, vol. 11, no. 3, pp. 355–361, Jul. 1966.

[26] G. Fiengo, D. G. Lui, A. Petrillo, S. Santini, and M. Tufo, "Distributed robust PID control for leader tracking in uncertain connected ground vehicles with V2V communication delay," *IEEE/ASME Transactions on Mechatronics*, vol. 24, no. 3, pp. 1153–1165, 2019.

[27] F. Gao, S. E. Li, Y. Zheng, and D. Kum, "Robust control of heterogeneous vehicular platoon with uncertain dynamics and communication delay," *IET Intelligent Transport Systems*, vol. 10, no. 7, pp. 503–513, 2016.

[28] R. Rajamani, *Vehicle Dynamics and Control* (MES), 2nd ed. Boston, MA: Springer, 2012, p. 498.

[29] D. He, T. Qiu, and R. Luo, "Fuel efficiency-oriented platooning control of connected nonlinear vehicles: A distributed economic MPC approach," *Asian Journal of Control*, vol. 22, no. 4, pp. 1628–1638, 2019.

[30] Y. Zheng, S. E. Li, K. Li, F. Borrelli, and J. K. Hedrick, "Distributed model predictive control for heterogeneous vehicle platoons under unidirectional topologies," *IEEE Transactions on Control Systems Technology*, vol. 25, no. 3, pp. 899–910, 2017.

[31] Z. Huang, Z. Chen, Y. Xu, C. Liu, and P. Shi, "Distributed Receding Horizon Estimation for Time Invariant Discrete Time Linear Systems Based on Substate Decomposition," *IEEE Transactions on Network Science and Engineering*, vol. 13, pp. 1071–1083, 2026.

[32] H. Rao, L. Zhao, Y. Xu, Z. Huang, and R. Lu, "Quasisynchronization for neural networks with partial constrained state information via intermittent control approach," *IEEE Transactions on Cybernetics*, vol. 52, no. 9, pp. 8827–8837, 2021.

[33] M. Segata, R. Lo Cigno, T. Hardes, J. Heinovski, M. Schettler, B. Bloessl, C. Sommer, and F. Dressler, "Multi-technology cooperative driving: An analysis based on PLEXE," *IEEE Transactions on Mobile Computing*, vol. 22, no. 8, pp. 4792–4806, Aug. 2023.

[34] M. Segata, L. Ghiro, and R. Lo Cigno, "On the progressive introduction of heterogeneous CACC capabilities," in *IEEE VNC 2021*, IEEE, Nov. 2021.

[35] J. M. Kennedy, J. Heinovski, D. E. Quevedo, and F. Dressler, "Centralized model-predictive control with human-driver interaction for platooning," *IEEE Transactions on Vehicular Technology*, vol. 72, no. 10, pp. 12 664–12 680, Oct. 2023.

[36] S. Melzer and B. Kuo, "Optimal regulation of systems described by a countably infinite number of objects," *Automatica*, vol. 7, no. 3, pp. 359–366, May 1971.

[37] M. Jovanovic and B. Bamieh, "On the ill-posedness of certain vehicular platoon control problems," *IEEE Transactions on Automatic Control*, vol. 50, no. 9, pp. 1307–1321, Sep. 2005.

[38] U. Nations, *Vienna Convention on Road Traffic*, https://globalautoregs.com/rules/157-1968-vienna-convention-on-road-traffic, 1968.

[39] A. Alam, A. Gattami, K. H. Johansson, and C. J. Tomlin, "Guaranteeing safety for heavy duty vehicle platooning: Safe set computations and experimental evaluations," *Control Engineering Practice*, vol. 24, pp. 33–41, Mar. 2014.

[40] UN Economic Commission for Europe, "Uniform provisions concerning the approval of motor vehicles with regard to the Advanced Emergency Braking Systems (AEBS)," 2014. [Online]. Available: https://unece.org/fileadmin/DAM/trans/main/wp29/wp29regs/2015/R131r1e.pdf.

[41] B. D. O. Anderson and J. B. Moore, *Optimal Filtering*. Upper Saddle River, NJ: Prentice Hall, 1979.

[42] M. S. Amjad, M. Schettler, S. Dimce, and F. Dressler, "Inband full-duplex relaying for RADCOM-based cooperative driving," in *IEEE VNC 2020*, IEEE, Dec. 2020.

[43] C. Ayimba, M. Segata, P. Casari, and V. Mancuso, "Closer than close: MEC-assisted platooning with intelligent controller migration," in *ACM MSWiM 2021*, Nov. 2021.

[44] C. Liu, H. Rao, X. Yu, Y. Xu, and C.-Y. Su, "State estimation for recurrent neural networks with intermittent transmission," *IEEE Transactions on Cybernetics*, vol. 54, no. 5, pp. 2891–2900, 2023.

[45] K. J. Åström and B. Wittenmark, *Computer-Controlled Systems: Theory and Design*, 3rd ed. Upper Saddle River, NJ: Prentice Hall, 2011, p. 557.

[46] B. Sinopoli, L. Schenato, M. Franceschetti, K. Poolla, M. Jordan, and S. Sastry, "Kalman filtering with intermittent observations," *IEEE Transactions on Automatic Control*, vol. 49, no. 9, pp. 1453–1464, Sep. 2004.

[47] D. E. Quevedo, A. Ahlén, A. S. Leong, and S. Dey, "On Kalman filtering over fading wireless channels with controlled transmission powers," *Automatica*, vol. 48, no. 7, pp. 1306–1316, Jul. 2012.

[48] G. Dimitrakopoulos and P. Demestichas, "Intelligent transportation systems," *IEEE Vehicular Technology Magazine*, vol. 5, no. 1, pp. 77–84, 2010.

[49] J. B. Rawlings, D. Q. Mayne, M. Diehl, et al., *Model predictive control: theory, computation, and design*. Nob Hill Publishing Madison, WI, 2020, vol. 2.

[50] R. Scattolini, "Architectures for distributed and hierarchical model predictive control–a review," *Journal of process control*, vol. 19, no. 5, pp. 723–731, 2009.

[51] D. E. Quevedo, A. Ahlen, and K. H. Johansson, "State estimation over sensor networks with correlated wireless fading channels," *IEEE Transactions on Automatic Control*, vol. 58, no. 3, pp. 581–593, 2012.

[52] M. Segata, F. Dressler, and R. Lo Cigno, "Jerk beaconing: A dynamic approach to platooning," in *IEEE VNC 2015*, Kyoto, Japan: IEEE, Dec. 2015, pp. 135–142.

[53] T. Keviczky, F. Borrelli, and G. J. Balas, "Decentralized receding horizon control for large scale dynamically decoupled systems," *Automatica*, vol. 42, no. 12, pp. 2105–2115, 2006.

BIOGRAPHIES

Justin M. Kennedy (Member, IEEE) received the B. Eng (Electrical)/B. Maths, and Ph.D. degrees in estimation and control of marine craft in the presence of environmental disturbances from the Queensland University of Technology (QUT), Brisbane, QLD, Australia, in 2016 and 2022, respectively. He was a Postdoctoral Researcher with the School of Electrical Engineering and Robotics, QUT. His research interest include the application of mathematical and control system tools to solve network engineering problems. Dr. Kennedy is a member of the IEEE Control Systems Society (CSS) and Society for Industrial and Applied Mathematics (SIAM).

Lixin Yang received the B.S. and Ph.D. degree in control science and engineering from the School of Automation, Guangdong University of Technology, Guangzhou, China, in 2018 and 2023, respectively. He is currently a Research Fellow with the Department of Electrical and Computer Engineering, National University of Singapore. He was a Postdoctoral Fellow with Queensland University of Technology and the Hong Kong Polytechnic University from 2023 to 2025. He was a visiting internship student with the Hong Kong University of Science and Technology. His research interests include networked control systems, cyber-physical security, and reinforcement learning.

Daniel E. Quevedo (Fellow, IEEE) received Ingeniero Civil Electrónico and MSc degrees from Universidad Técnica Federico Santa María, Valparaíso, Chile, in 2000, and in 2005 the PhD degree from the University of Newcastle, Australia. Since 2024 he has been Professor of Electrical and Computer Engineering at The University of Sydney. Prior to his current appointment he served as a faculty at Queensland University of Technology in Brisbane and at Paderborn University, Germany. In 2003 he received the IEEE Conference on Decision and Control Best Student Paper Award and was also a finalist in 2002. He is co-recipient of the 2018 IEEE Transactions on Automatic Control George S. Axelby Outstanding Paper Award. Prof. Quevedo currently serves as Associate Editor for *IEEE Control Systems*, for *IEEE Transactions on Control of Network Systems* and on the Editorial Board of the *International Journal of Robust and Nonlinear Control*. From 2015–2018 he was Chair of the IEEE Control Systems Society Technical Committee on Networks & Communication Systems. His research interests are in networked control systems, control of power converters and cyber-physical systems security.

Falko Dressler (Fellow, IEEE) received the M.Sc. and Ph.D. degrees from the Department of Computer Science, University of Erlangen, Erlangen, Germany, in 1998 and 2003, respectively. He is currently a Full Professor and Chair of Telecommunication Networks with the School of Electrical Engineering and Computer Science, TU Berlin, Berlin, Germany. His research interests include adaptive wireless networking (sub-6GHz, mmWave, visible light, molecular communication) and wireless-based sensing with applications in ad hoc and sensor networks, the Internet of Things, and Cyber-Physical Systems. Dr.Dressler is also an Associate Editor-in- Chief of IEEE TRANSACTION ON MOBILE COMPUTING and Elsevier Computer Communications and the Editor of journals such as IEEE/ACM TRANSACTION ON NETWORKING, IEEE TRANSACTION ON NETWORK SCIENCE AND ENGINEERING, Elsevier Ad Hoc Networks, and Elsevier Nano Communication Networks. He has been Chairing conferences such as IEEE INFOCOM, ACM MobiSys, ACM MobiHoc, IEEE Vehicular Networking Conference (VNC), IEEE GLOBECOM. He authored the textbooks Self-Organization in Sensor and Actor Networks published by Wiley&Sons and Vehicular Networking published by Cambridge University Press. He has been an IEEE Distinguished Lecturer and an ACM Distinguished Speaker. Dr. Dressler is an ACM Distinguished Member. He is the Member with the German National Academy of Science and Engineering (acatech). He has been serving on the IEEE COMSOC Conference Council and the ACM SIGMOBILE Executive Committee.